BRIGHAM YOUNG UNIVERSITY

GEOLOGY STUDIES

Volume 20: Part 4 — December 1973

CONTENTS

Brigham Young University Geology Studies

Volume 20, Part 4—December, 1973

Contents

A publication of the
Department of Geology
Brigham Young University
Provo, Utah 84602

Brigham Young University Geology Studies is published semiannually by the department. *Geology Studies* consists of graduate-student and staff research in the department and occasional papers from other contributors. *Studies for Students* supplements the regular issues and is intended as a series of short papers of general interest which may serve as guides to the geology of Utah for beginning students and laymen.

Distributed December 19, 1973

Price $5.00

Mica Pyroxenite Inclusions in Limburgite, Hopi Buttes Volcanic Field, Arizona*

Paul H. Lewis
Brigham Young University, Provo, Utah

ABSTRACT.—Analyses of black, mica-amphibole-clinopyroxene inclusions and associated megacrysts and phenocrysts from a dike and diatremes of the Hopi Buttes volcanic field, Arizona, reveal that the clinopyroxene is titanaugite with 5.4 to 10.8% Ca-Tschermak molecule, that the mica is titanium-rich phlogopite, and that the amphiboles are pargasites and kaersutites.

Large, euhedral, nonzoned titanaugite phenocrysts of the limburgite tuff of the diatremes have a composition essentially equivalent to those of the megacrysts and the corresponding phase of the inclusions, implying that all are cognate precipitates.

Hypothetical parental melts of the limburgite magma can be estimated from the data on the inclusions and limburgite and can be used to define fractionation trends for the limburgite. On the basis of these trends, fractionation is concluded not to have played any significant role in the development of the limburgite. These trends also indicate that the limburgite and monchiquite of the field are not genetically related.

CONTENTS

*A thesis submitted to the faculty of the Department of Geology, Brigham Young University, in partial fulfillment of the requirements for the degree Master of Science.

INTRODUCTION

Northeastern Arizona may be subdivided into two general volcanic provinces (Text-fig. 1). The Navajo volcanic field is a potassium-rich minette province in the extreme northeastern portion of the state. It is Oligocene in age, giving radiometric dates of 31 million years (Naeser, 1971), and is characterized by plugs and diatremes.

The Hopi Buttes volcanic field is a sodium-rich monchiquite province in the Hopi Indian Reservation and the southern part of the Navajo Indian Reservation. It consists of numerous flows, dikes, and diatremes, and is Pliocene in age, 2 to 5.5 million years (Naeser, 1971).

Diatremes of these two fields have not been investigated in detail on a chemical and petrological basis. Hack (1942) conducted a general study of the regional volcanism, but no chemical data were presented. Williams (1936) published a reconnaissance study with 17 analyses on the general petrology of the two fields. He suggested that a common source of magma could have generated the two volcanic fields if sufficient crustal contamination occurred in the Navajo field to produce the high potassium content. On the grounds of a petrologic study, Nicholls (1969) concluded that the rock suite of one field could not have been derived from the other by crystal fractionation. The different ages for the two fields make any genetic connection between them unlikely.

Uranium occurrences in the diatremes of the Hopi Buttes field have been treated by Shoemaker (1955) and Lowell (1956).

Ultramafic inclusions have been reported from both fields. Watson (1967) describes the kimberlitic pipes of the Navajo field but offers no explanation for their origin. McGretchin (1968) describes kimberlite of the Moses Rock dike and interprets it as being "derived mechanically from physically disaggregated spinel- and garnet-peridotite in the mantle." All ultramafic inclusions (clinopyroxite, eclogite, websterite, and lherzolite) are thought to be accidental inclusions from the vent walls.

Few ultramafic inclusions have been reported in the Hopi Buttes field. Some consisting of amphibole and varying amounts of diopsidic augite and phlogopite have been described as "crystal lapilli" (Williams, 1936).

Over the years many hypotheses have been presented explaining the nature and origin of such ultramafic inclusions. The major ones are as follows:

1. The inclusions represent primordial mantle material.
2. They are a residuum of partial melting of the primordial mantle.
3. They are cumulate products of crystal settling in magmas of some earlier period.
4. They are the product of crystal settling in the magmas which produced

the host rock now enclosing the inclusions, i.e., they are cognate precipitates (Kuno and Aoki, 1970).

Garnet and spinel iherzolite inclusions of rather constant composition with high Mg/Fe ratios are believed to be pieces of the primordial mantle from which basaltic melts can be derived by partial melting.

Lherzolite suites with lower Mg/Fe ratios and relatively substantial variation of the major elements are interpreted as residua of partial fusion of mantle peridotite (Kuno and Aoki, 1970).

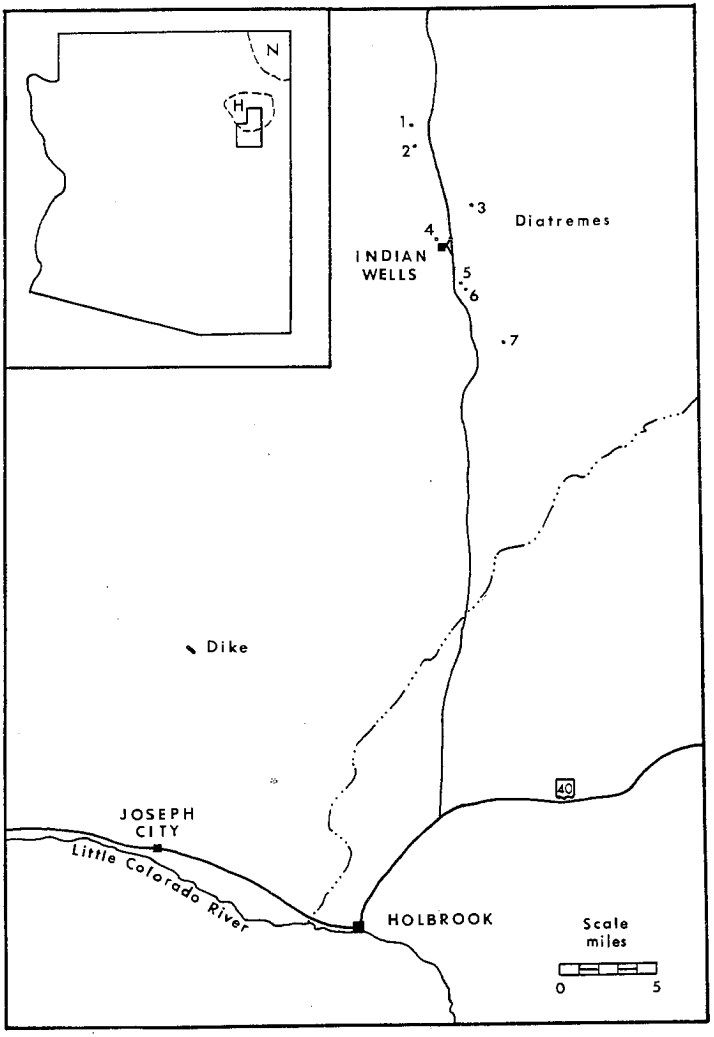

TEXT-FIGURE 1.—Index map showing location of dike and diatremes in study area. Insert shows location of study area within state (solid line), of the Hopi Buttes field (dashed line, H), and of the Navajo volcanic field, (dashed line, N).

Inclusions that crystallized in a magma of some earlier period and were "accidentally" incorporated by a later melt are difficult to distinguish from cognate precipitates. Detailed geochemical data on the inclusions and host rock phases, however, should be useful in distinguishing between the two.

Waters (1955) points out similarities between the Hopi Buttes rocks and alkalic ultramafic lavas from Uganda that contain abundant inclusions of biotite pyroxenite. He suggests that the Uganda inclusions may be metamorphic rocks formed by biotitization of orogenic serpentinites, pyroxenites, and amphibolites that were later caught up by a melt and partially resorbed or melted by the host magma. Opposed to this, Holmes (1950) and Higazy (1954) interpret the inclusions as cognate precipitates.

The only plutonic inclusions in this study of the Hopi Buttes field are mica-amphibole clinopyroxenites with igneous textures. The objective of the project is to determine the compositions and the origin of the inclusions and their relation to the limburgite host rock.

Results will not only provide pertinent information on these particular inclusions but will also aid in the interpretation of similar inclusions from other regions.

ACKNOWLEDGMENTS

Coverage of operational expenses for the electron microprobe through N. S. F. Grant GA-15082 to M. G. Best is deeply appreciated. Sincere thanks are extended to those who aided in the project, especially W. P. Nash of the University of Utah for assistance in operating the electron microprobe and M. G. Best for suggestions and general assistance.

FIELD RELATIONS

Volcanic rocks of the Hopi Buttes are contemporaneous with the Pliocene Bidahochi Formation that was deposited on the Hopi Buttes erosional surface. The Bidahochi Formation consists of interbedded volcanic tuffs and calcareous sandstone, the product of extensive interaction between volcanic eruptions and epiclastic events in Lake Bidahochi. Many eruptions occurred within the lake itself. Subsequent erosion has dissected the Bidahochi and underlying formations and some of the lava flows, leaving the region spotted with flow-capped mesas in addition to dikes, plugs, and diatremes. Diatremes were emplaced by upward drilling and explosion of gas-rich magma. Because of magma withdrawal or escape of gases, collapse has sometimes followed eruption, producing a local basin. Diatremes with the largest diameter occur where erosion has been slow. The degree of dissection of the diatremes in the province increases from north to south. Throughout the field the diatremes and dikes have a definite northwest-southeast trend (Hack, 1942).

One dike and seven diatremes were investigated for this project. Text-figure 1 shows their location. Of these localities only the dike and diatreme 2 yielded ultramafic inclusions.

Dike

On the extreme southern margin of the Hopi Buttes volcanic field, 13 miles north of Joseph City, a 4,000-foot-long dike rises 25 to 30 feet above the sparsely vegetated valley of Cottonwood Wash. The dike consists of black limburgite and dips about 80° to the southwest. Outcrops form an *en echelon* pat-

tern. The undisturbed nature of the country rock in the immediate vicinity indicates that *en echelon* outcrop pattern was predetermined by a fracture system in the host Triassic Chinle Formation and Triassic-Jurassic Glen Canyon Group rather than by post-emplacement faulting.

The dike ranges from a few inches to two feet in thickness and displays a pervasive horizontal joint system presumably related to cooling. This feature is well exposed on the southeast end of the dike where a small arroyo has eroded some of the sand and alluvial deposits that everywhere obscure the dike-country rock contact.

Two feeder plugs in the center of the dike are 80 feet high and consist of agglomerate which contains large sandstone and siltstone xenoliths of the Chinle Formation. There is no sign of alteration in these xenoliths.

Diatremes

The diatremes are centrally located within the Hopi Buttes volcanic field and lie within an eight-mile radius of Indian Wells, Navajo County. The diatremes can be divided into two categories: maar diatremes and vent diatremes.

Diatremes 2, 3, and 5 are of the first category and consist of abundant light gray to olive green tuffaceous rock comprised of poorly sorted and unconsolidated clasts. Layers of boulder conglomerate and some limburgite are interbedded with tuff. Thinly bedded units of fine-grained limestone or calcareous shales cap the tuff. Distinct bedding is inclined towards the center of the structure, which is generally circular and has a diameter up to 1,500 feet. The dip of these units is usually 10° or less except along the flanks where the dip may be as much as 75°. The maar diatremes are easily eroded and have low topographic profiles.

The vent diatremes (1, 4, 6, and 7) are comprised of successive, roughly horizontal layers of limburgite that vary from 10 to 50 feet in thickness. This layering probably represents multiple eruptions occurring over a short period of time. Vertical columnar jointing is sometimes present in the upper layers. Only minor tuffaceous rock is present. The vent diatremes have a greater topographic relief. They rise abruptly 100 feet or more above the present surface, presenting a black, craggy silhouette against the sky and red country rock. They are circular in outline and have a diameter of up to 400 feet. Around their perimeters, sand and talus slides conceal contacts with the country rock.

PETROGRAPHY

Samples were collected from the dike and all the diatremes except number 5. Inclusions were present in the dike and diatreme 2. Megacrysts were only found in the dike.

Limburgite Host Rock

Limburgite comprises 90% or more of the dike and the vent diatremes and about 5 to 10% of the maar diatremes. The limburgite is black and usually porphyritic. Phenocrysts, where present, consist of variably zoned titaniferous augite and of olivine and lie in a dark brown, glassy matrix containing abundant microlites of augite, equidimensional spinel, and, rarely, minute olivine (Plate 1, fig. 1). Up to 5% aragonite is present as fillings of vesicles and other cavities. Accessory minerals are hematite, fluorite, serpentine, and iron oxides. No feldspars or feldspathoids were found in any sample. Augite phenocrysts

range from 1 to 6 mm. In hand specimen they are black and in thin section, transparent with a light tinge of green. The crystals are usually strongly zoned, and their cores are characterized by fractures, cavities, and small areas altered to pleochroic amphibole and mica. Olivine phenocrysts are the same size as those of augite and are locally altered to iddingsite. They are usually equidimensional and euhedral; some are H-shaped.

Limburgite from the various localities differs primarily in the phenocryst-matrix ratio and in the proportion of augite, glass, and spinel in the matrix. Table 1 summarizes these differences.

The major rock type of the maar diatremes is a coarse medium gray to olive green tuff. Large, euhedral nonzoned phenocrysts of black (in hand sample) augite constitute 10 to 20% of the tuff, and they vary in size from 0.5 to 2 cm. Plate 1, figs. 2 and 3). Rare mica flakes less than 4 mm. are present.

The black augite phenocrysts in the tuff have well-developed crystal faces and probably grew as free floating entities in a liquid environment. Front and side pinacoids together with [110] and [011] prisms are fully developed. Cleavage on [110] is poor, and contact twinning on [110] is present. The crystal faces are typified by numerous small, irregular pits. In thin section the phenocrysts are a light pastel green and have a spongy texture around the margin. Their interiors are fractured and contain many cavities.

The large size and lack of zoning distinguish the augite phenocrysts of the tuff from the smaller ones of the limburgite.

TABLE 1
MODAL COMPOSITION OF REPRESENTATIVE SAMPLES OF LIMBURGITE

	Phenocrysts				Matrix				
	total	in rock	augite	olivine	total	in rock	glass	augite	spinel	olivine
Dike		10	50	50		85	45	35	20	1
Diatremes										
1		19	80	29		80	35	45	20	
2		10	100			87	55	30	15	
3		10	50	50		88	40	45	15	
4		15	50	50		84	40	45	15	1
6						100	30	55	15	
7		15	95	5		85	25	55	20	

EXPLANATION OF PLATE 1
LIMBURGITE AND PHENOCRYSTS OF HOPI BUTTES

FIG. 1.—Limburgite from dike viewed in plane light. Opaque grains are ulvospinel, prisms with high relief are augite in a glass matrix, and white region in lower center is microphenocryst of augite.

FIG. 2.—Augite phenocrysts from diatreme 3; larger crystal is 6.5 mm. in [100] direction, 5.0 mm. in the [010], and 5.0 mm. in the [001].

FIG. 3.—Augite phenocrysts from tuff of diatreme 3, 10.5 mm. in the [100] direction, 10.0 mm. in the [010]; and 12.5 mm. in the [001].

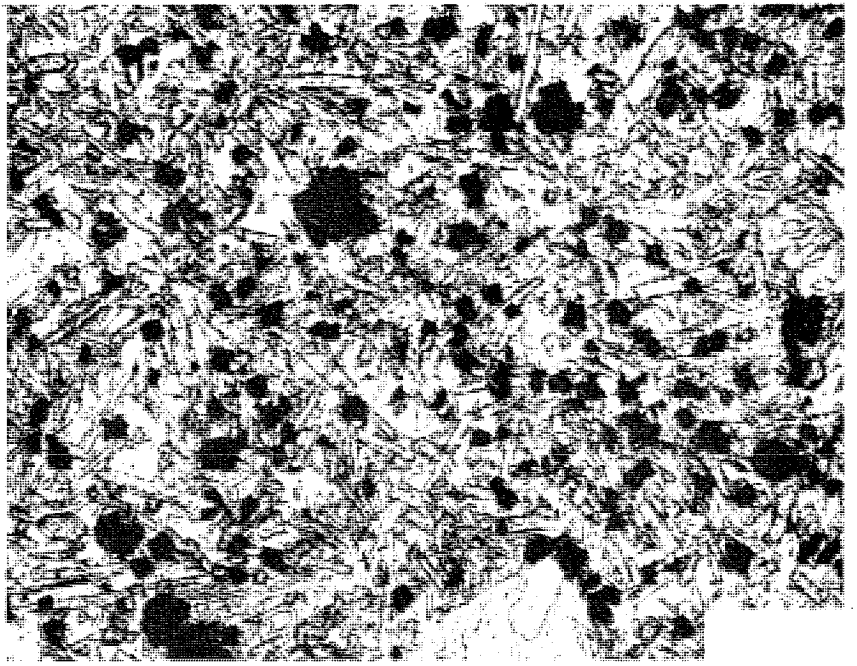

1

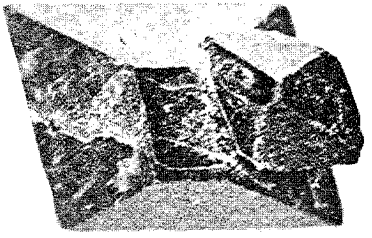

2

3

PLATE 1

Megacrysts

The limburgite of the dike contains about 3% megacrysts of anhedral clinopyroxene and amphibole and subhedral mica. Upon detailed inspection some megacrysts are found to contain very small grains of a second phase. In view of this, the distinction between megacrysts and inclusions is sometimes arbitrary.

About 90% of the megacrysts are clinopyroxene. They are anhedral, have very poor cleavage, and are optically homogeneous. Their size ranges from 1 to 5 cm., and they have fractured interiors with cavities and small areas altered to amphibole and mica. They are black in hand specimen but transparent with a light greenish hue in thin section. Outer margins commonly display a spongy texture.

Micas comprise about 5% of the megacrysts. They are subhedral and optically homogeneous with straw-yellow to dark coffee-brown pleochroism. Spinel-rich haloes in the limburgite host envelope these grains. The micas are 1 to 3 cm.

Anhedral amphiboles constitute 5% of the megacrysts and range from 1 to 5 cm. Pleochroism is straw-yellow to dark honey-brown. [110] cleavage is well defined, and haloes rich in spinel often surround the grains.

Inclusions

About 2% of the dike is comprised of mica-amphibole clinopyroxenite inclusions. No lherzolite inclusions have been found. Text-figure 2 shows the modal composition of 59 inclusions. They range from 1 to 5 cm., and all are phaneritic and hypocrystalline. Intergranular material in the inclusions closely resembles the host rock and consists of glass with microlites of augite and spinel. As much as 3% of an inclusion may consist of cavities filled with aragonite. These ovoidal cavities are 1 to 3 mm. and may lie between grains or entirely within a single mineral grain. In one instance aragonite has precipitated along cleavage planes in a grain of mica. Serpentine and unidentifiable mineral grains are locally present in a carbonate filled cavity (Plate 5, fig. 2).

Black clinopyroxene of the inclusions is very pale green in thin section. Subtle hour-glass zoning is present in the grains of perhaps 20% of the inclusions. Their interiors are also characterized by fractures, cavities, very minute "bubbles," and small patches of amphibole and mica. Individual grains range from 3 cm. to less than 1 mm.

EXPLANATION OF PLATE 2
PHOTOMICROGRAPHS OF INCLUSIONS

FIG. 1.—Phlogopite clinopyroxenite, diatreme 2. Augites are medium gray, darker grains are phlogopite; $CaCO_3$ fills small cavities. Augite-c, phlogopite-p, and $CaCO_3$-cc. Inclusion is 4 cm. across.

FIG. 2.—Websterite, inclusion E of diatreme 2.5 cm. across. Euhedral pheochroic bronzite (b) dominates; minor anhedral augite is present (c); gray to dark gray grains enclosing small anhedra of bronzite are phlogopite (p); small black grains at lower right are spinel; $CaCO_3$ (cc) invades phlogopite. Voids are cavities and plucked grains.

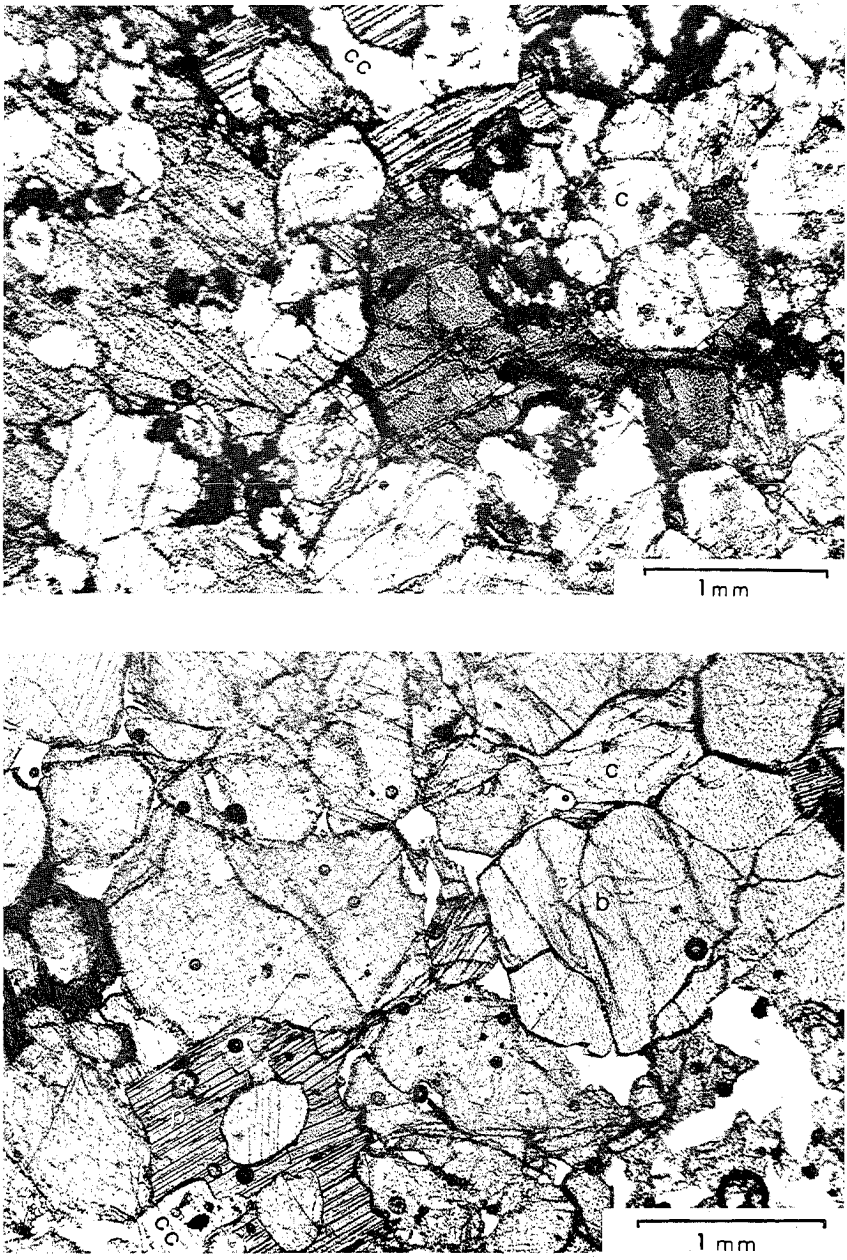

2

PLATE 2

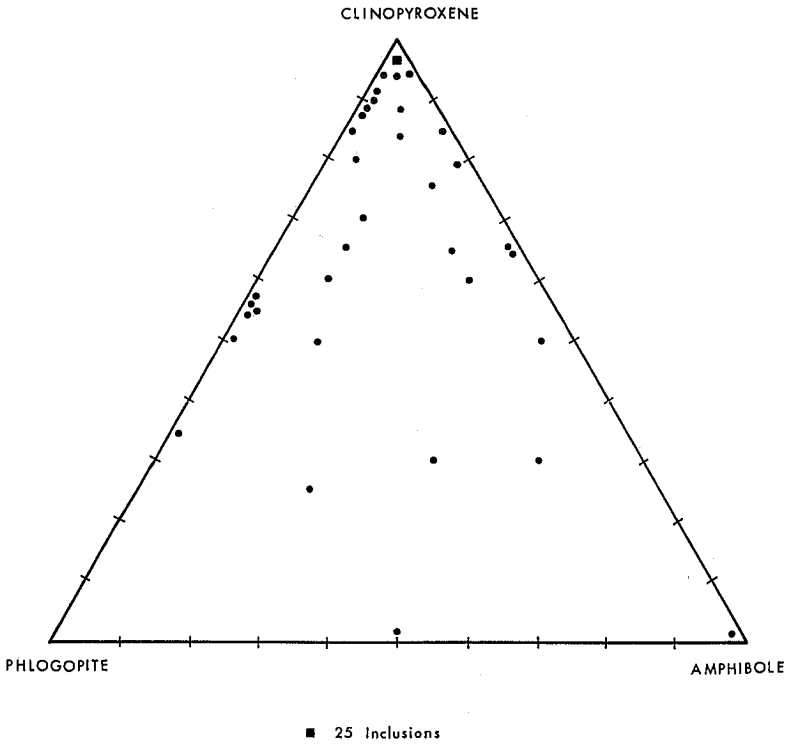

TEXT-FIGURE 2.—Modal composition of 59 inclusions from dike; intergranular glass, augite and spinel seldom exceed 1% and are not shown.

Mica and amphibole in the inclusions are similar to the megacrysts and range from 0.5 mm. to 2 cm.

Clinopyroxene, mica, and amphibole are usually combined in hypidiomorphic, poikilitic, or cataclastic textures, in order of decreasing abundance, and are described below:

Hypidiomorphic: Mineral grains are equant to subequant; subhedral mica is common as an interstitial filling between euhedral to anhedral grains of clinopyroxene (Pl. 2, figs. 1 and 2). Some areas of the inclusions appear granoblastic, but the polygonal habit of this texture is not pervasive and many grains are euhedral. Plate 3, figure 1 shows anhedral mica which surrounds and fills embayments in anhedral clinopyroxene.

Poikilitic: Oikocrysts of mica and amphibole enclose grains of subhedral to anhedral clinopyroxene as in Plate 3, figure 2 and Plate 4, figure 1. An interesting variant of this texture is shown in Plate 4, figure 2, wherein all the clinopyroxene grains are uniformly oriented and belong to a large, 4 cm., homogeneous crystal. On a reduced scale all the micas look deceptively like an oikocryst enclosing the clinopyroxene grains. In some instances (Pl. 5, fig. 1) interstitial amphibole jackets sinuous blebs of mica.

Cataclastic: Fractured and crenulated mica grains predominate. Clinopyroxene may or may not be strained. Amphibole is absent from these inclusions.

Inclusions from diatreme 2 are mica clinopyroxenites and have weathered out of the coarse tuff. The inclusions comprise approximately 1% of the tuff and are normally coated with a very thin layer of limburgite. They range from 2 to 10 cm. They are holocrystalline and have a hypidiomorphic or poikilitic texture. These textures are the same as those of the inclusions from the dike, and the occurrence of aragonite is the same. Text-figure 3 gives the modal composition of 29 inclusions.

One websterite inclusion was found at diatreme 2. It has a hypidiomorphic texture. The orthopyroxene is euhedral and ranges from about 0.1 to 3 mm. The pleochroism is light straw-yellow to very faint pinkish brown. The 1% (or less) spinel is black, opaque, and is euhedral to subhedral. Anhedral clinopyroxene and mica are similar to those of the other inclusions.

ANALYTICAL PROCEDURE

Whole-rock analyses were made with the electron microprobe, following a method outlined by Rucklidge, Gibb, Fawcett, and Gasparrini (1970). The samples were trimmed, cleaned, crushed, and hand picked to remove secondary

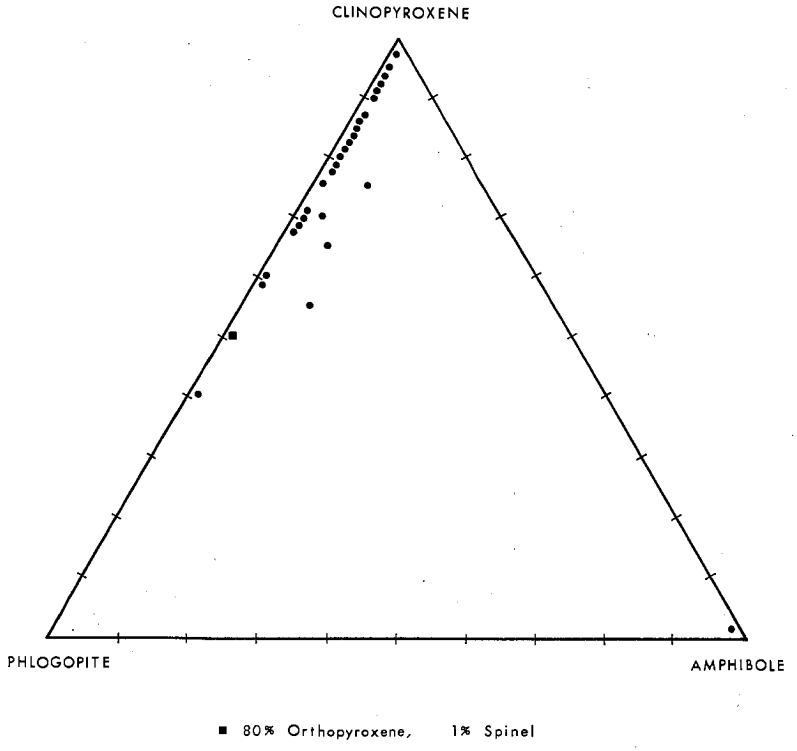

TEXT-FIGURE 3.—Modal composition of 29 inclusions from diatreme 2.

carbonate. They were next pulverized to pass a 150 mesh and, if necessary, bathed in a lukewarm solution of dilute HCl to dissolve any remaining carbonate. Samples were fused in a graphite crucible utilizing a platinum-wound furnace to which was attached a vacuum system to remove water vapor created during fusion. Fusion was between 1,250 and 1,300°C for 10 to 15 minutes. After quenching, the samples were examined with a petrographic microscope to see if fusion was complete. Although analyses with the microprobe revealed that the glasses were not entirely homogeneous, this was partially compensated for by utilizing a large beam diameter of 20 microns, moving the beam across the glass during counting, and making 10 integrations of about 10 seconds each.

Precision standard 1 (Brimhall and Embree, 1971) was analyzed by this technique as a test of precision and accuracy. Results are shown in Table 2.

All mineral phases of the inclusions were analyzed with a 0.05 microampere sample current; a 0.03 microampere current was used for the glasses. An integrated beam current count of 40,000 was employed for all analyses with 15 kilovolts of power. The raw data were entered into a computer program (Rucklidge, 1967 with modification by G. McKay and I. S. McCallum), and all compositional data have been taken from the computer printout. The minerals were more homogenous than the glasses. Values for ferric iron, where present, were determined from calculations on the charge balance and molecular proportions in the mineral assuming that iron was the only multi-valent element present. The composition of clinopyroxene in terms of the end member molecules was computed after the method of Kushiro (1962). The atomic formula for clinopyroxene is based on three oxygens, and the one for amphibole, on 23.

CHEMISTRY

Scrutiny of the compositions of the megacrysts, crystalline phases of the limburgite, tuff, and inclusions will be important in determining the genetic links between them. Data on the limburgite and tuff will be presented first, then that of the megacrysts and inclusions.

TABLE 2
PRECISION STANDARD 1

	A	B
SiO_2	47.83 ± 0.14	47.91 ± 0.86
TiO_2	1.94 0.02	1.99 0.13
Al_2O_3	16.08 0.03	15.11 0.38
FeO	10.94 0.07	11.17 0.08
MnO	0.17 0.01	nd
MgO	8.96 0.05	8.85 ± 0.10
CaO	9.12 0.03	9.01 0.42
Na_2O	3.39 0.02	3.20 0.05
K_2O	1.52 0.01	1.49 0.05

A - Microprobe, 90% confidence interval in percentage. B - Atomic absorption, average of six analysis, 90% confidence interval in percentage, (Brimhall and Embree, 1971). Total iron as Fe.

Host Rocks

Chemical and normative compositions of the limburgite from the dike and diatremes 2 and 4 are listed in Table 3. Ferric iron and water were not analyzed. The rocks are silica undersaturated and are rich in titanium and alkalies. Normative nepheline ranges from 4.3 to 13.8%. Normative olivine is higher than it would be if some ferric iron were present in the analyses. Based on normative composition, these rocks are similar to basanites and olivine poor nephelinites (Green and Ringwood, 1967; Bultitude and Green, 1971) with the feldspathoidal constituents occult in the glass.

Tables 4, 5, and 6 give the compositions of various phases of the limburgite. These data show that the high titanium content of the rock is contributed largely by ulvospinel with 19.4 to 22.5 wt. % TiO_2. The sodium is contributed mainly by the glass, and the calcium and magnesium are contained primarily in the clinopyroxene. The glass is rich in silicon, aluminum, and alkalies.

The clinopyroxene is titanaugite with high concentrations of CaO. Partial analysis of the groundmass augite, indicates, as expected, that it has the same composition as the rims of the zoned phenocrysts in the limburgite. From core to rim of the phenocrysts, the (100 Mg/Fe + Mg) atomic ratio decreases substantially, and the Ca-Tschermak molecule is reduced to zero. Aluminum in phenocryst rims and groundmass augite fills tetrahedral sites. In groundmass augite the amount of tetrahedral aluminum varies inversely as the silica concentration of the magma (LeBas, 1962). Comparison of the host-rock composition of the dike and diatreme 4 with the rim of augite phenocrysts in the respective rocks shows that they conform to the above observation. Substitution of tetrahedral aluminum for silicon creates a charge deficiency in the pyroxene which may be compensated for by the addition of ferric iron or titanium. Kushiro (1960) suggests that the titanium content of the host rock does not determine the amount of tetrahedral aluminum in the pyroxene structure but that it only enters in order to maintain electrostatic neutrality.

TABLE 3
WHOLE ROCK ANALYSIS

	1	2	3		1	2	3
SiO_2	42.50	44.95	43.81	or	6.56	9.00	7.05
TiO_2	3.69	5.20	4.44	ab	4.50	12.50	1.51
Al_2O_3	12.21	10.70	11.22	ne	13.83	4.25	14.52
FeO	12.74	12.16	12.25	an	13.82	22.10	20.04
MnO	0.40	0.21	0.20	di	33.40	23.25	27.27
MgO	7.92	6.81	8.39	ol	15.62	14.00	16.52
CaO	13.58	12.88	13.00	il	7.05	9.86	8.45
Na_2O	3.61	2.48	3.71	ap	4.06	4.00	3.69
K_2O	1.11	1.47	1.39				
P_2O_5	1.53	1.51	1.46				
Total	99.29	98.86	98.87				

1 - Limburgite, dike, Navajo Co., Arizona. Average of four analyses. 2 - Limburgite, diatreme 2, block from vent, Navajo Co., Arizona. 3 - Limburgite, diatreme 4, lava filling in vent, Navajo Co., Arizona. Total iron as FeO.

TABLE 4
PHASES OF DIKE HOST ROCK

	1							2			
	Phenocrysts			Matrix				Phenocrysts		Matrix	
	clinopyroxene		olivine	spinel	augite	olivine	glass	augite	olivine	augite	olivine
	core	rim									
SiO_2	48.33	43.20		0.14			54.72				
TiO_2	1.16	3.98		19.38			0.52				
Al_2O_3	5.37	7.50		5.17			24.37				
Cr_2O_3				0.83							
Fe_2O_3	5.23	6.60		25.68							
FeO	1.86	1.92	12.90*	43.81	8.02*	17.71*	2.13*	7.22*	13.08*	8.20*	18.85*
MgO	14.59	11.83	44.01	3.90	11.48	40.49	0.93	14.14	43.80	12.50	42.79
CaO	19.82	22.96	0.33	0.54	22.20	0.45	5.54	21.77	0.31	21.78	0.25
Na_2O	1.20	0.60		0.04			7.93				
K_2O	0.01	0.01		0.07			2.89				
Total	98.33	98.66		99.56			99.03				
$\frac{100\ Mg}{Fe + Mg}$	80	73	86	10	72	80	45	78	86	73	80
Si	.905	.822		0.00	$En_{35.9}$			$En_{39.5}$		$En_{35.3}$	
AlIV	.095	.168			$Fs_{14.1}$			$Fs_{13.8}$		$Fs_{15.0}$	
Al^{VI}	.024			0.02							
Cr				0.02	$Wo_{50.0}$			$Wo_{46.7}$		$Wo_{49.7}$	
Fe^{+3}	.073	.093		0.69							
Ti	.016	.057		0.53							
Fe^{+2}	.030	.032		1.30							
Mg	.407	.336		0.21							
Ca	.398	.469		0.02							
Na	.044	.022									

1 - Euhedral augite phenocryst weathered out of tuff, diatreme 1. 2 - Euhedral augite phenocryst weathered out of tuff, diatreme 3. 3 - Limburgite from diatreme 4. * - Total iron as FeO. F_2O_3 calculated.

TABLE 5
PHASES OF DIATREME HOST ROCK

	1	2	3						
			Phenocrysts					Matrix	
			clinopyroxene		olivine	spinel	augite	olivine	glass
			core	rim					
SiO_2	49.48	50.08	49.41	45.09	39.32	1.68			55.34
TiO_2	1.41	1.16	1.49	3.46	0.03	22.59			0.77
Al_2O_3	5.97	4.77	5.77	6.39	0.07	3.70			24.86
Fe_2O_3	4.05	4.38	4.20	6.60	1.38	20.06			
FeO	3.28	2.22	2.74	1.73	15.34	43.76	7.85*	17.24*	1.72*
MnO	0.15	0.15	0.14	0.11	0.21	0.79			0.10
MgO	15.36	15.91	14.32	12.51	44.03	6.47	12.03	40.99	1.13
CaO	19.05	19.72	20.89	23.61	0.29	0.93	23.51	0.38	5.75
Na_2O	1.11	1.05	1.11	0.55	0.02	0.10			7.66
K_2O	0.03	0.04	0.03	0.00	0.02	0.10			1.31
Total	99.89	99.48	100.10	100.05	100.71	99.18			98.64
$\frac{100\ Mg}{Fe + Mg}$	80	82	80	74	83	15	73	81	55
Si	.908	.921	.908	.845	.986	.059	$En_{36.1}$		
Al^{IV}	.092	.079	.092	.141	.002				
Al^{VI}	.037	.025	.033			.154	$Fs_{13.2}$		
Fe^{+3}	.056	.061	.058	.093	.026	.531	$Wo_{50.7}$		
Ti	.019	.016	.021	.049	.001	.598			
Fe^{+2}	.051	.034	.042	.027	.322	1.259			
Mn	.002	.002	.002	.002	.004	.024			
Mg	.420	.436	.392	.349	1.648	.340			
Ca	.374	.388	.411	.474	.008	.035			
Na	.040	.037	.039	.020	.002				

1 - Limburgite enclosing inclusion B. 2 - Limburgite enclosing inclusions F.* - Total iron as FeO. F_2O_3 calculated.

TABLE 6
MOLECULAR END MEMBER PROPORTIONS FOR
CLINOPYROXENE PHENOCRYSTS OF HOST ROCKS

	1	1'	2	3	4	4'
$NaFe^{+3}Si_2O_6$	8.7	4.4	7.9	7.5	7.9	4.0
$CaTiAl_2O_6$	3.3	10.5	3.9	3.2	4.1	9.8
$CaFe^{+3}AlSiO_6$	5.9	10.8	3.3	4.7	3.7	11.6
$CaAl_2SiO_6$	5.6		7.4	4.8	6.5	
$Ca_2Si_2O_6$	32.4	35.8	30.1	32.5	34.0	36.7
$Mg_2Si_2O_6$	40.7	33.6	42.0	43.6	39.2	34.9
$Fe_2^{+2}Si_2O_6$	3.0	5.0	5.0	3.4	4.2	2.7

1 - Core, from limburgite enclosing inclusion B of dike, see Table 4. 1' - Rim of 1. 2 - Diatreme 1, see Table 5. 3 - Diatreme 3, see Table 5. 4 - Core, from limburgite of diatreme 4, see Table 5. 4' - Rim of 4.

The direct relation between silica content of the pyroxene and silica concentration in the magma may be valid for groundmass augite, but the presence of 5 wt. % more SiO_2 in the core than the rim of the phenocrysts cannot be attributed to a change of silica concentration in the melt, since the residual melt (now interstitial glass) has 12% more SiO_2 than the whole rock. In this case low pressures as opposed to elevated ones seem to favor large proportions of tetrahedral aluminum in augite.

The large euhedral unzoned phenocrysts from the tuff are similar in composition to the cores of the small zoned phenocrysts in the limburgite with 4.8 to 7.4 mol. % Ca-Tschermak molecule.

Megacrysts and Inclusions

Three clinopyroxene megacrysts and the major phases of thirteen inclusions were analyzed. The megacryst data are listed in Table 7. Since their compositions are about the same as that of the clinopyroxene from the inclusions, they will be treated together.

The thirteen inclusions are from the dike and diatreme 2 and consist of clinopyroxenites, two amphibole rocks, and one websterite. Clinopyroxenes are the most abundant phase of the inclusions, and relevant chemical data are presented in Tables 8 and 9. They are sodium-rich, aluminous titanaugites. The total oxide weight varies from 99.18 to 100.77% with ferric iron calculated and included. Chromium content, where analyzed, is low, which is typical of clinopyroxene from black-pyroxene inclusions (Ishibashi, 1970). The (100 Mg/Fe + Mg) ratio ranges from 69 to 85 and averages a little higher for the augite of diatreme 2 than for that of the dike. Aluminum content varies inversely with silicon and directly with titanium and is partitioned between tetrahedral and with octahedral sites in the clinopyroxene-solid solution. Octahedral aluminum permits the formation of the Ca-Tschermak and jaedite molecules. Ca-Tschermak molecule ranges from 5.3 to 10.8 mol. % and averages 7.6% Interestingly, the augite from the diatreme 2 amphibole rock has the largest per-

TABLE 7
CLINOPYROXENE MEGACRYSTS FROM DIKE

	A	B	C
SiO_2	49.29	50.08	48.95
TiO_2	1.35	1.24	1.42
Al_2O_3	5.86	5.62	6.44
Fe_2O_3	4.38	3.10	3.14
FeO	3.31	3.24	3.97
MnO	0.16	0.13	0.15
MgO	14.30	15.39	14.50
CaO	19.41	19.79	19.47
Na_2O	1.34	1.02	1.17
K_2O	0.04	0.04	0.03
Total	99.44	99.65	99.26
Si	.911	.919	.905
Al^{IV}	.089	.081	.095
Al^{VI}	.039	.041	.045
Fe^{+3}	.061	.043	.044
Ti	.019	.017	.020
Fe^{+2}	.051	.050	.061
Mn	.003	.002	.002
Mg	.394	.421	.399
Ca	.384	.389	.386
Na	.048	.036	.042
K	.001	.001	.001
$NaFe^{+3}Si_2O_6$	9.6	7.3	8.4
$CaTiAl_2O_6$	3.8	3.4	4.0
$CaFe^{+3}AlSiO_6$	2.6	1.3	0.3
$CaAl_2SiO_6$	7.7	8.1	9.9
$Ca_2Si_2O_6$	31.4	32.5	31.4
$Mg_2Si_2O_6$	39.4	42.1	39.9
$Fe^{+2}_2Si_2O_6$	5.1	5.0	6.1
$\frac{100\ Mg}{Fe + Mg}$	78	82	79

A - Size 1 cm, from southeast part of dike. B - Size 4 cm., from center of dike. C - Size 4 cm., from northwest part of dike. Fe_2O_3 calculated.

TABLE 8
CLINOPYROXENES FROM INCLUSIONS OF DIKE

	A	B	C	D	E	F	G
SiO_2	50.00	48.89	50.18	47.89	49.28	51.00	50.90
TiO_2	1.14	1.54	1.21	1.66	1.44	0.88	0.92
Al_2O_3	5.00	6.25	4.85	6.34	6.78	4.49	5.04
Cr_2O_3	nd	0.09	nd	0.03	nd	nd	nd
Fe_2O_3	5.25	3.92	6.60	6.33	2.94	5.85	1.53
FeO	2.32	3.59	2.66	2.77	4.12	3.57	5.68
MnO	0.20	0.13	0.18	0.15	0.16	0.28	0.15
MgO	14.06	13.46	12.11	12.65	14.16	12.53	15.01
CaO	20.04	20.06	20.13	20.20	19.09	19.09	19.23
Na_2O	1.60	1.36	2.25	1.59	1.31	2.37	1.21
K_2O	0.05	0.00	0.04	0.01	0.05	0.04	0.04
Total	99.66	99.18	100.21	99.62	99.33	100.11	99.71
Si	.992	.907	.928	.892	.910	.941	.934
Al^{IV}	.078	.093	.072	.109	.090	.059	.066
Al^{VI}	.031	.043	.033	.031	.057	.039	.043
Cr	nd	.001	nd	.001	nd	nd	nd
Fe^{+3}	.073	.044	.092	.089	.041	.081	.021
Ti	.016	.021	.017	.023	.020	.020	.013
Fe^{+2}	.036	.056	.043	.043	.064	.055	.087
Mn	.003	.002	.003	.002	.003	.004	.002
Mg	.387	.373	.334	.351	.390	.345	.411
Ca	.396	.399	.399	.402	.378	.377	.378
Na	.057	.049	.080	.047	.047	.085	.043
K	.001	.000	.001	.000	.001	.001	.001
$NaFe^{+3}Si_2O_6$	11.4	9.8	16.1	11.5	8.2	16.3	4.2
$NaAlSi_2O_6$					1.2	0.7	4.4
$CaTiAl_2O_6$	3.2	4.3	3.4	4.6	4.0	2.5	2.5
$CaFe^{+3}AlSiO_6$	3.1	1.1	2.2	6.2			
$CaAl_2SiO_6$	6.1	8.8	6.1	6.2	10.2	7.0	6.1
$Ca_2Si_2O_6$	33.4	32.8	34.5	31.7	30.7	33.0	33.4
$Mg_2Si_2O_6$	38.7	37.3	33.4	35.1	39.0	34.5	41.1
$Fe^{+2}_2Si_2O_6$	3.6	5.6	4.1	4.3	6.2	5.5	8.7
$\frac{100\ Mg}{Fe + Mg}$	78	77	71	73	79	72	79

A - Pargasite-phlogopite clinopyroxenite, southeast portion of dike. B - Phlogopite-kaersutite clinopyroxenite, southeast portion of dike. C - Pargasite clinopyroxinite, southeast portion of dike. D - Phlogopite-clinopyroxene amphibole rock, center section of dike. E - Phlogopite clinopyroxenite, center section of dike. F - Phlogopite clinopyroxenite, center section of dike. G - Clinopyroxenite, northwest segment of dike. Fe_2O_3 calculated.

TABLE 9
CLINOPYROXENES FROM THE INCLUSIONS OF DIATREME 2

	A	B	C	D	E	E'	F
SiO_2	49.17	50.54	49.87	49.74	50.05	50.54	50.48
TiO_2	1.22	1.20	1.34	1.07	1.25	1.16	1.22
Al_2O_3	5.96	4.75	6.00	6.39	6.07	5.68	5.08
Fe_2O_3	5.16	3.87	4.29	5.69	3.92	3.18	3.93
FeO	1.82	3.44	2.54	4.59	3.63	4.26	1.93
MnO	0.14	0.17	0.16	0.25	0.17	0.18	0.13
MgO	15.03	14.86	15.40	12.26	15.58	15.37	16.61
CaO	20.22	20.25	19.65	18.36	17.85	18.10	19.89
Na_2O	1.14	1.15	1.16	2.17	1.38	1.36	0.90
K_2O	0.04	0.05	0.04	0.04	0.04	0.04	0.04
Total	99.79	100.28	100.45	100.57	99.94	99.87	100.21
Si	.903	.926	.909	.916	.915	.925	.918
Al^{IV}	.097	.074	.091	.084	.085	.075	.082
Al^{VI}	.032	.029	.038	.054	.046	.048	.027
Fe^{+3}	.074	.053	.059	.079	.054	.044	.054
Ti	.017	.017	.018	.015	.017	.016	.017
Fe^{+2}	.025	.053	.039	.071	.056	.065	.028
Mn	.002	.003	.002	.004	.003	.003	.002
Mg	.411	.406	.418	.336	.435	.420	.450
Ca	.396	.398	.384	.362	.350	.355	.388
Na	.041	.041	.041	.078	.049	.048	.032
K	.001	.001	.001	.001	.001	.001	.001
$NaFe^{+3}Si_2O_6$	8.1	8.2	8.2	15.5	9.8	8.8	6.4
$NaAlSi_2O_6$						0.9	
$CaTiAl_2O_6$	3.4	3.3	3.7	3.0	3.4	3.2	3.3
$CaFe^{+3}AlSiO_6$	6.7	2.5	3.5	0.3	1.0		4.4
$CaAl_2SiO_6$	6.2	5.7	7.4	10.8	9.2	8.6	5.3
$Ca_2Si_2O_6$	31.5	34.0	31.0	29.2	28.2	29.6	32.2
$Mg_2Si_2O_6$	41.4	40.6	41.9	33.6	42.5	42.0	45.1
$Fe^{+2}_2Si_2O_6$	2.5	5.3	3.9	7.2	6.0	6.5	2.8
$\frac{100\ Mg}{Fe + Mg}$	81	79	81	69	80	79	85

A - Phlogopite clinopyroxenite. B - Phlogopite-pargasite clinopyroxenite. C - Phlogopite clinopyroxenite, minor serpentine. D - Clinopyroxene amphibole rock. E - Phlogopite websterite. E' - Different region of E. F - Phlogopite clinopyroxenite. Fe_2O_3 calculated.

TABLE 10
PHLOGOPITES FROM INCLUSIONS
Letters of samples correspond to those of Tables 8 and 9. Total iron as FeO.

	Dike					Diatreme 2					
	A	B	D	E	F	A	B	C	E	E'	F
SiO_2	36.56	35.29	35.11	36.65	35.89	36.30	36.70	36.64	36.99	36.65	36.98
TiO_2	5.31	6.74	7.07	6.85	5.79	6.93	6.24	6.88	7.28	7.15	7.11
Al_2O_3	15.47	16.05	15.79	16.38	15.16	15.95	15.93	15.96	15.92	15.99	16.30
Cr_2O_3	0.12	0.09	0.03	nd	nd	nd	nd	nd	nd	nd	nd
FeO	10.22	11.00	12.24	9.17	13.46	9.37	10.96	9.64	8.66	8.86	8.60
MnO	0.07	nd	nd	0.07	0.15	0.07	0.09	0.06	0.06	0.07	0.05
MgO	17.21	15.79	15.01	16.08	15.15	17.01	16.76	16.81	16.64	16.56	17.38
CaO	0.21	0.24	0.22	0.20	0.19	0.16	0.14	0.17	0.17	0.15	0.17
Na_2O	0.93	0.86	0.84	0.85	0.83	0.63	0.78	0.87	0.55	0.55	0.72
K_2O	9.31	8.80	8.80	9.43	9.31	9.83	9.61	9.71	10.30	10.16	9.70
Total	95.41	94.85	95.11	96.40	95.91	96.25	97.22	96.74	96.57	96.14	97.00
$\frac{100\ Mg}{Fe + Mg}$	75	72	69	77	67	77	73	76	78	77	78

TABLE 11
AMPHIBOLES FROM INCLUSIONS
Letters of samples correspond to those of Tables 8 and 9. Total iron as FeO.

	Dike				Diatreme 2	
	A	B	C	D	B	D
SiO_2	41.10	40.23	40.46	39.69	41.57	41.14
TiO_2	3.84	4.71	3.92	4.93	3.65	4.51
Al_2O_3	12.24	13.43	12.68	13.15	12.61	13.31
Cr_2O_3	0.13	0.10	nd	0.03	nd	nd
FeO	9.87	10.06	12.23	11.20	10.65	12.40
MnO	0.20	0.15	0.17	0.15	0.16	0.15
MgO	14.59	13.41	12.46	12.74	14.49	12.31
CaO	10.70	10.96	10.48	11.03	10.20	10.12
Na_2O	2.97	2.54	3.05	2.55	2.97	2.70
K_2O	1.89	2.03	1.89	2.06	1.76	2.18
Total	97.73	97.63	97.36	97.64	98.06	98.81
$\frac{100\ Mg}{Fe + Mg}$	72	70	64	71	71	64
Si	6.071	5.959	6.059	5.920	6.109	6.053
Al^{IV}	1.929	2.043	1.941	2.080	1.891	1.947
Al^{VI}	.238	.301	.298	.231	.294	.364
Cr	.017	.011	nd	.003	nd	nd
Ti	.427	.524	.441	.553	.404	.499
Fe	1.219	1.247	1.532	1.398	1.308	1.526
Mn	.025	.018	.021	.018	.018	.020
Mg	3.213	2.961	2.783	2.855	3.175	2.699
Ca	1.693	1.740	1.681	1.763	1.606	1.595
Na	.851	.730	.886	.739	.847	.770
K	.356	.384	.362	.392	.331	.409

centage of Ca-Tschermak molecule and the lowest (100 Mg/Fe + Mg) ratio. Jaedite molecule, if present, is less than 5 mol. %, and the highest sodium contents are found in the clinopyroxene with relatively large amounts of ferric iron.

The second most abundant phase of the inclusions is mica. Ten of the thirteen inclusions contain mica, and eleven grains were analyzed. Analyses are given in Table 10. On the basis of the Mg/Fe atomic ratios, the mica is phlogopite (Deer, Howie, and Zussman, 1966). The oxide totals range from 94.85 to 97.22%. Lack of information on water and fluorine accounts in part for the low totals. A number of analyses on phlogopite from inclusions (Aoki and Kushiro, 1968) reveal that water and fluorine vary from 2 to 5 wt. %, so these totals are within tolerable limits. If ferric iron were added this would also increase the totals by a few tenths of one percent. The phlogopites are very rich in titanium, and the (100 Mg/Fe + Mg) ratios range from 67 to 78, again averaging slightly higher for diatreme 2.

Amphibole occurs in six of the analyzed inclusions and is the least abundant phase. Amphibole analyses are tabulated in Table 11. The oxide totals range from 97.36 to 98.84%. Low totals are again due to lack of data on water, ferric iron, and fluorine. Based on a systematic classification for calciferous and subcalciferous amphiboles devised by Leake (1968), these are pargasites and kaersutites. The distinction between the two is specified by the formula content of titanium. If titanium in the molecular formula is more than 0.50, the amphibole is kaersutite; if it is less than 0.50, it is pargasite. For the sake of simplicity, both will hereafter be referred to as amphibole. The (100 Mg/Fe +

TABLE 12
ORTHOPYROXENE FROM INCLUSION OF DIATREME 2

	E	E'
SiO_2	54.21	53.72
TiO_2	0.16	0.33
Al_2O_3	3.54	4.02
Fe_2O_3	0.63	1.41
FeO	10.87	10.30
MnO	0.22	0.22
MgO	29.37	28.90
CaO	1.23	1.31
Na_2O	0.12	0.16
K_2O	0.02	0.02
Total	100.37	100.39
$\frac{100\ Mg}{Fe + Mg}$	82	82
Si	.954	.948
Al^{IV}	.046	.052
Al^{VI}	.028	.031
Fe^{+3}	.008	.019
Ti	.002	.004
Fe	.160	.152
Mn	.003	.003
Mg	.771	.760
Ca	.023	.025
Na	.004	.005
K	.000	.000

Letters of samples correspond to those of Table 9. F_2O_3 calculated.

Mg) ratios show a similar but lower range (64 to 72) when compared with the clinopyroxene and phlogopite.

Two grains of orthopyroxene were analyzed from the inclusion of websterite from diatreme 2. The pyroxene is aluminous bronzite (Deer, Howie, and Zussman, 1963), and Table 12 lists its composition.

Analysis of carbonate-filled cavities in the same inclusion revealed that they are 97% $CaCO_3$ with minor Mn, Fe, and Mg. Crystal habit indicates that the carbonate is aragonite.

ORIGIN OF INCLUSIONS

Pressure and Temperature Conditions

It is generally accepted that the Ca-Tschermak molecule in the clinopyroxene solid solution series is a physicochemical indicator of the pressures prevailing at the time of crystallization (Aoki et al., 1968; Clark, Schairer, and de Neufville, 1962; Ito and Kennedy, 1968; and Kushiro, 1965). Nonetheless, few if any data specify the exact percentage of the Ca-Tschermak molecule which corresponds to a given depth since its concentration is not a unique function of pressure. High pressure experimental data (Bultitude and Green, 1971) on crystallization of nephelinitic magmas show that coexisting aluminous phases, temperature, and the type of container used in the experiment affect the Ca-Tschermak molecule content in clinopyroxene under isobaric conditions.

Under isobaric and isothermal conditions, melts of differing compositions also precipitate clinopyroxene with varying percentages of the Ca-Tschermak molecule (Bultitude and Green, 1971). The uncertain influence of these combined variables on the content of Ca-Tschermak molecule in clinopyroxene is sufficient to preclude the assignment of a single, unique pressure for a given percentage of the molecule.

The Ca-Tschermak molecule content of the clinopyroxenes from the inclusions and megacrysts is compared in Text-figure 4 to that from other localities and is interpreted as indicating elevated pressures at the time of crystallization. That the percentage of Ca-Tschermak molecule in the clinopyroxene of one inclusion differed from that of the next may be the result of any of the variables mentioned above.

Attempts were made to calculate the total pressure at the time of crystallization of the inclusions by utilizing a thermodynamic procedure outlined by Nicholls, Carmichael, and Stormer (1971). However, as a test on the reliability of the procedure calculations on observed mineral compositions, temperatures, and pressures from experimental data (Bultitude and Green, 1971) on nephelinitic systems showed that the computed pressures varied as much as $\pm 30\%$ from the experimental values. On these grounds the procedure was deemed unsatisfactory in determining the pressure at the time of inclusion crystallization. Lack of experimental data on undersaturated, hydrous magmas similar to the Hopi Buttes limburgites makes it virtually impossible to assign a meaningful temperature-pressure range to conditions of crystallization of the inclusions.

Paragenesis

Textures indicate that the major mineral phases of the inclusions are primary, but since phlogopite and amphibole have been reported as secondary vein minerals with igneous-like textures, the possibility that these phases of the inclusions are secondary will be briefly considered.

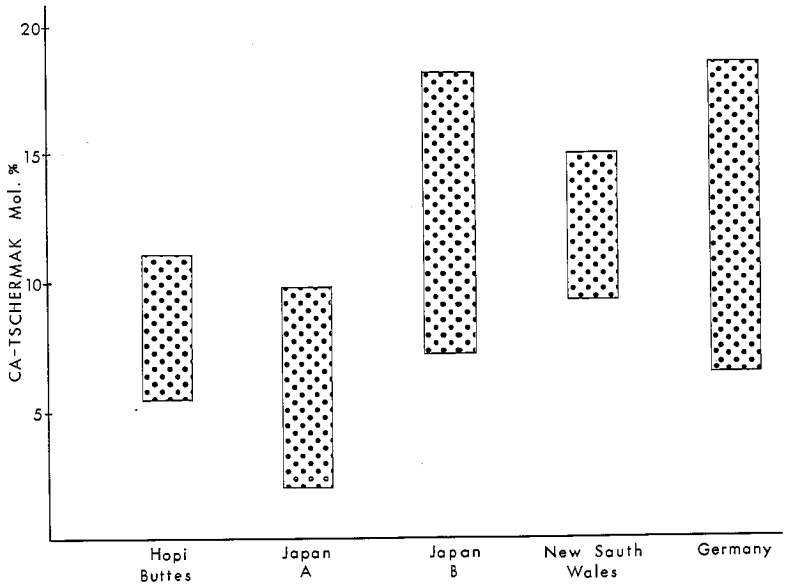

TEXT-FIGURE 4.—Comparison of the Ca-Tschermak molecule content of clinopyroxene in inclusions and megacrysts from the Hopi Buttes field with those from other localities. Japan-A, clinopyroxenes of peridotite inclusions from alkali olivine basalt (Kuno, 1964): Japan-B, clinopyroxene xenocrysts from alkali olivine basalt (Kuno, 1964); New South Wales, clinopyroxene megacrysts in alkaline lavas (Binns, Duggan, Wilkinson, 1970); Germany, clinopyroxenes from clinopyroxenite inclusions in basanite C, Aoki and Kushiro, 1968).

Lherzolites from Dish Hill, California, contain secondary amphibole and phlogopite as ascertained by veins of these hydrous minerals that transect anhydrous mineral grains, invade fractures of anhydrous mineral grains, and cut metamorphic foliations (Wilshire and Trask, 1971). In these lherzolites there is no textural evidence of a reaction relation between the hydrous and anhydrous phases. Inclusions from the Hopi Buttes include no lherzolite. The hydrous minerals in them are more abundant than those in the Dish Hill lherzolite, and the phlogopite is commonly poikilitic and fills embayments in the anhydrous minerals rather than transecting them. Some of the phlogopite and amphibole oikocrysts engulf anhedral clinopyroxene without invading any of their fractures. On the basis of these observations it is concluded that the hydrous mineral phases are not secondary but primary.

The textures illustrated in Plates 2, 3, and 4 suggest that there may have been a reaction relation between phlogopite and clinopyroxene during crystallization. The textural relations in Plate 5, figure 1 indicate the possibility of a similar reaction between phlogopite and amphibole. Based on textures alone the order of crystallization is orthopyroxene, clinopyroxene, phlogopite, and amphibole. Text-figure 5 shows a fractionation trend in phlogopite for FeO, MgO, and K_2O which with the coexisting phases support the order of crystallization as elucidated from the textures. Variation diagrams for amphibole with its coexisting phases supply only limited data, but they define the lower stability range of phlogopite. Clinopyroxene coexists with all other phases,

and amphibole and phlogopite coexist over a short range. With the relative stability fields of amphibole and phlogopite and of phlogopite and clinopyroxene overlapping, it is feasible that the reaction relations referred to on the basis of textures actually occurred.

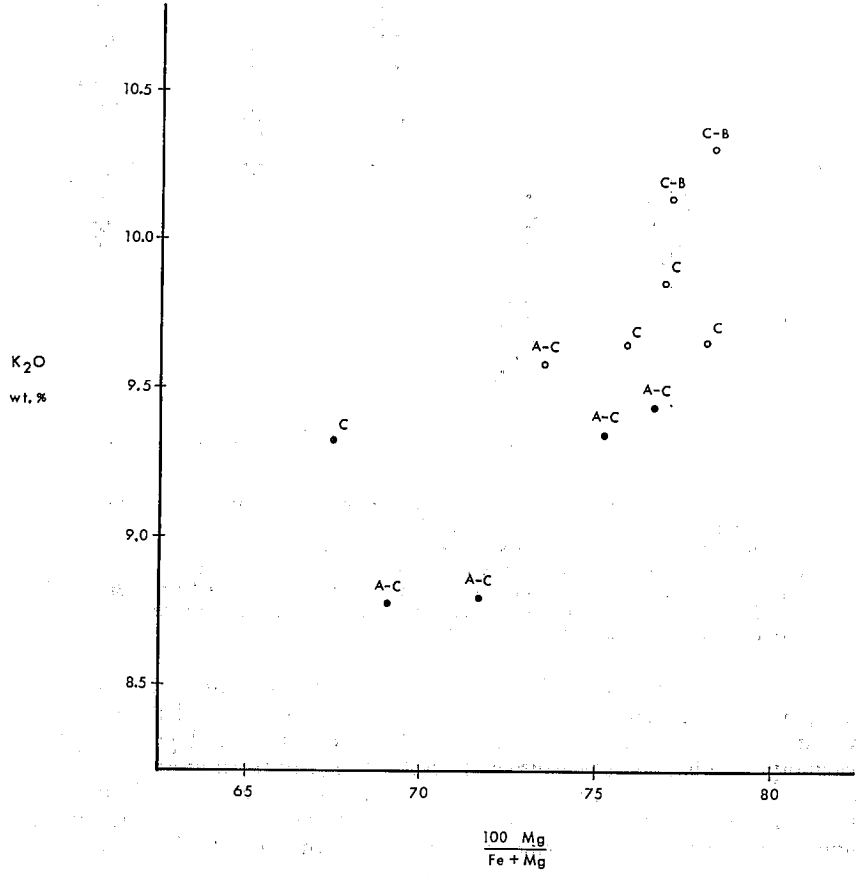

TEXT-FIGURE 5.—Variation diagram for the phlogopites of the inclusions. K_2O is plotted against the 100 Mg/Fe + Mg atomic ratio. Solid circles are phlogopites from the dike inclusions, open circles are phlogopites from the inclusions of diatreme 2. Coexisting phases are listed: amphibole-A, clinopyroxene-C, and bronzite-B.

EXPLANATION OF PLATE 3
PHOTOMICROGRAPHS OF INCLUSIONS

FIG. 1.—Phlogopite clinopyroxenite from dike, southeast portion. Dark phlogopite (p) fills embayments in augite (c); small cavity of $CaCO_3$ (cc) is intergranular; minute glass and spinel occur along grain boundaries. Size of inclusion is 2 cm.

FIG. 2.—Phlogopite clinopyroxenite, inclusion C of diatreme 2 (4 cm. in size). Phlogopite is dark (o), augite is light (c); some $CaCO_3$ (cc) filled cavities are entirely within grains of augite and phlogopite. Oikocryst of phlogopite surrounds cavity of $CaCO_3$ and grain of augite in lower left-hand corner.

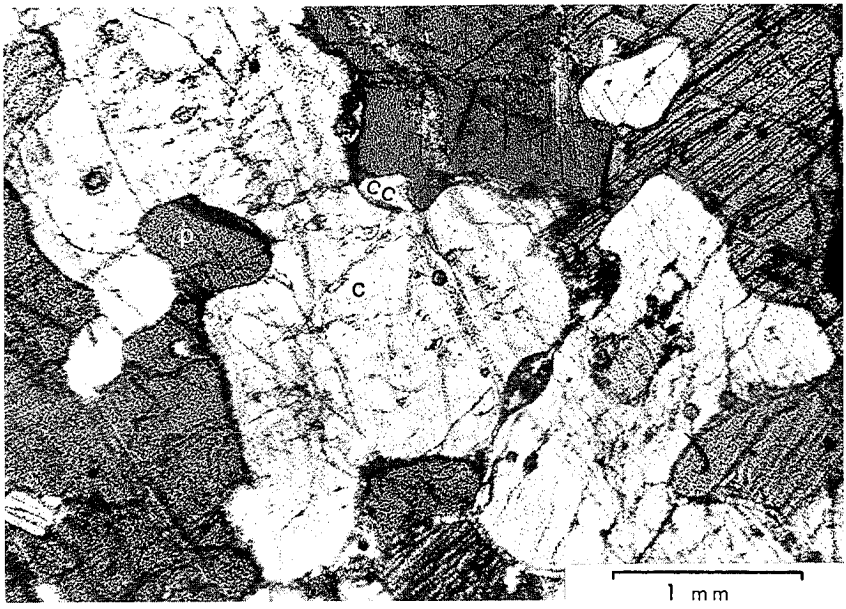

1

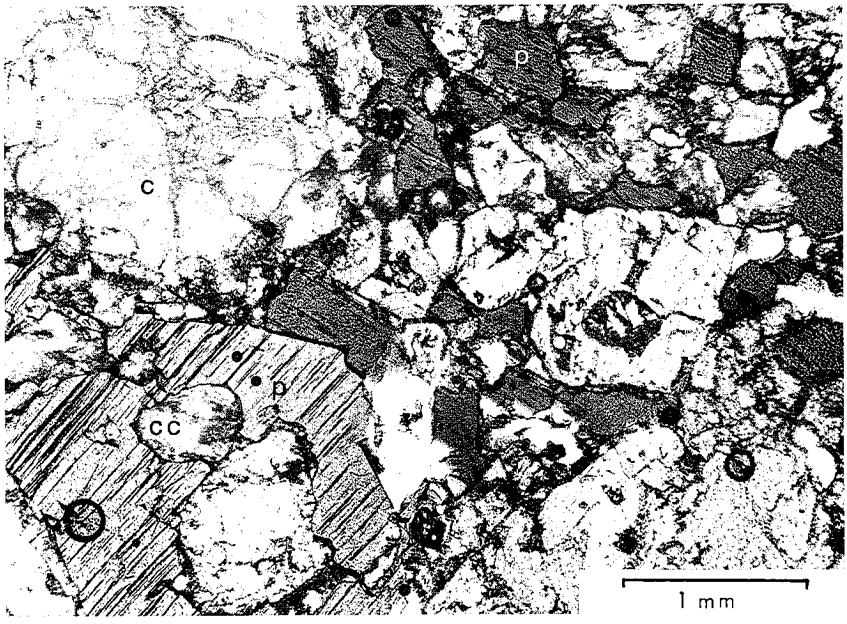

2

PLATE 3

Unfortunately, the significant fractionation trend with coexisting phases for the clinopyroxenes (Text-fig. 6) does not agree completely with the paragenesis of mineral phases as established above. The variation diagram of FeO, MgO, and Na_2O for the clinopyroxenes indicates that the orthopyroxene momentarily appeared in the paragenetic sequence well after phlogopite had begun to precipitate and not at the first of the sequence as the textures and var-

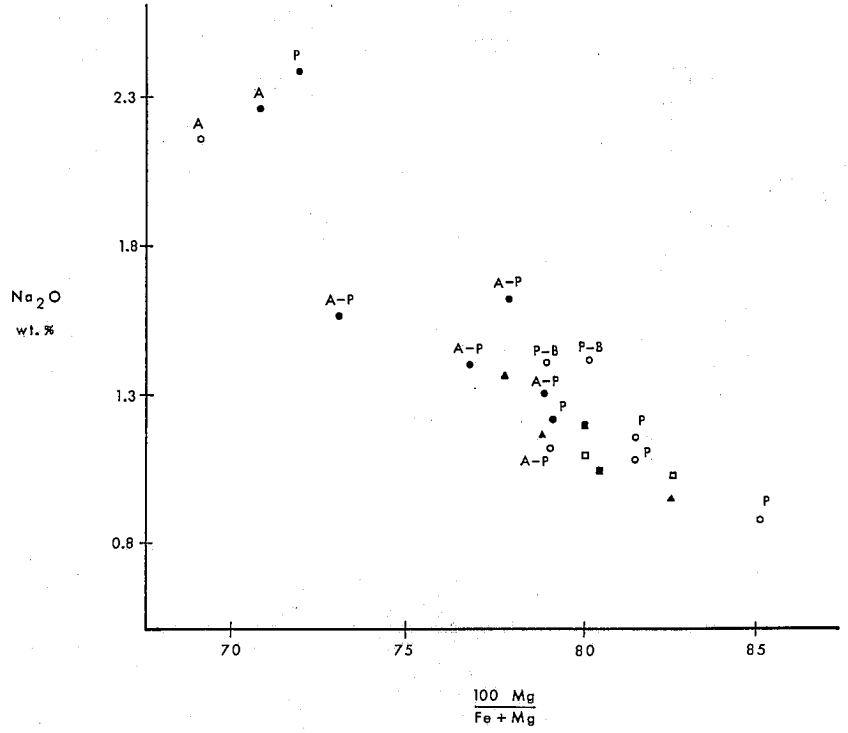

TEXT-FIGURE 6.—Variation diagram for the clinopyroxenes of the Hopi Buttes rocks. Na_2O is plotted again the 100 Me/Fe+M_2 atomic ratio. Solid circles are clinopyroxenes from the dike inclusions; open circles are clinopyroxenes from the inclusions of diatreme 2; solid triangles are the clinopyroxene megacrysts; open squares are the large euhedral, nonzoned augire phenocrysts; and the solid squares are the cores of the small zoned phenocrysts from the limburgite. Coexisting phases are listed: amphibole-A, phlogopite-P, and bronzite-B.

EXPLANATION OF PLATE 4
PHOTOMICROGRAPHS OF INCLUSIONS

FIG. 1.—Amphibole clinopyroxenite from dike. Oikocryst of amphibole (a) encloses subhedral grains of augite (c) and $CaCO_3$ (cc). Intergranular glass and spinel occur locally along margins of oikocryst. Size of inclusion is 1 cm.

FIG. 2.—Phlogopite clinopyroxenite, inclusion A of diatreme 2 (6 cm. in size). Crystallographically continuous, anhedral augites (c) enclosed by numerous grains of phlogopite (p) with prominent cleavage traces. Voids are plucked grains.

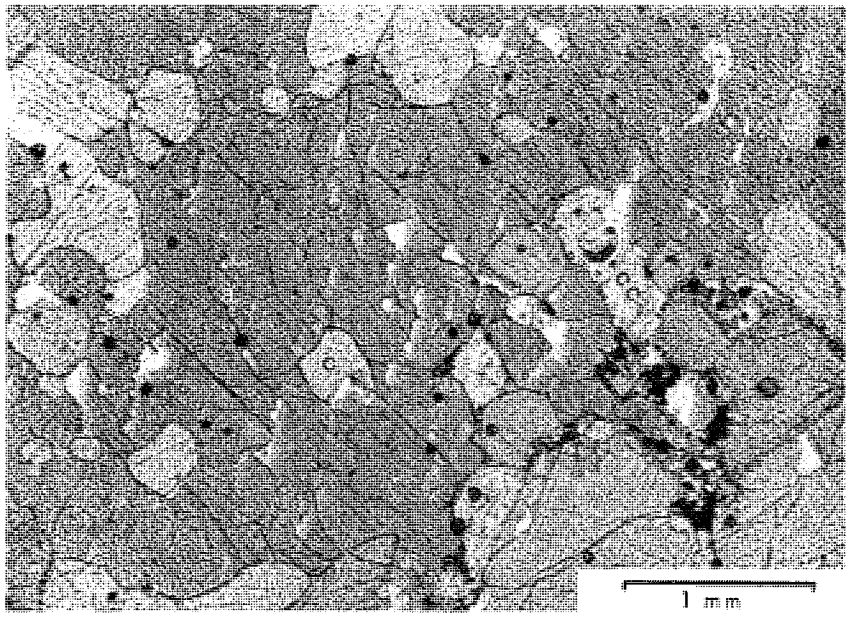

1

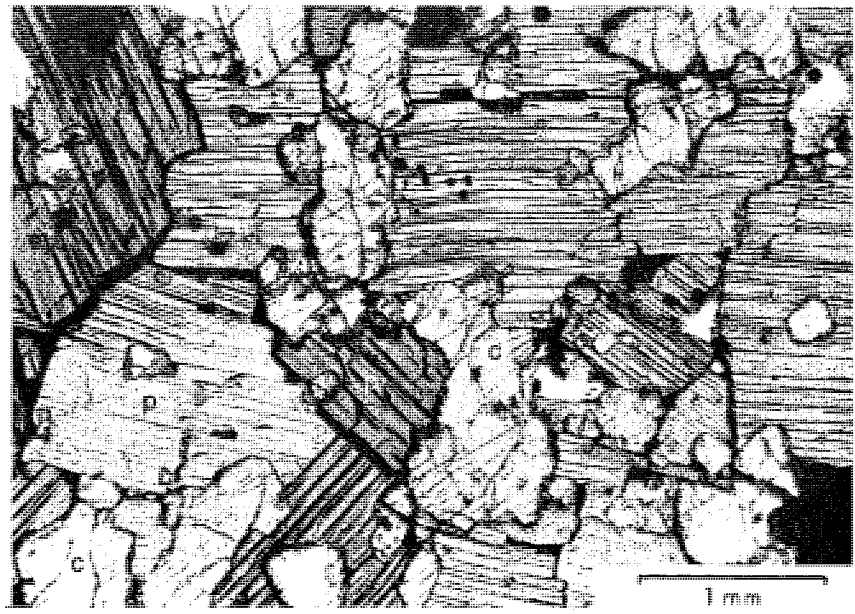

2

PLATE 4

iation diagram for phlogopite indicate. This discrepancy cannot be explained in terms of the available data. It is possible that the websterite (inclusion E of diatreme 2) is foreign to the suite of inclusions, but this seems doubtful considering the close correlation of the clinopyroxene and phlogopite in the websterite with the corresponding phases in the other inclusions.

On the basis of coexisting phases there is one other inclusion (F of the dike) which is anomalous in the variation diagram for phlogopite and clinopyroxene. Lack of amphibole (the anomaly) may be attributed to its small size (1 cm.) which makes it unrepresentative of the larger body from which it came. If this is not true, the inclusions may be foreign to the suite.

Noncognate versus Cognate Origin

As pointed out in the introduction, various hypotheses have been expounded for the origin of ultramafic inclusions. These will be discussed one at a time.

Primordial mantle material is believed to be lherzolite with high Mg/Fe ratios (Kuno and Aoki, 1970). No lherzolite inclusions were found in this study.

The residuum after partial melting is also lherzolite but is considered to possess lower Mg/Fe ratios and larger chemical variations than primary mantle lherzolite as a result of varying degrees of partial melting (Kuno and Aoki, 1970). The Mg/Fe ratios of the Hopi Butte inclusions are relatively low, and the mineralogy is incompatible with lherzolite. On this basis, these inclusions are not residua of partial melting.

The textures of the inclusions indicate that they are of igneous origin. The rare inclusions with cataclastic texture probably represent local deformation prior to eruptive processes. Intergranular glass, augite, and spinel in the hypocrystalline inclusions resemble the limburgite matrix very closely and probably resulted from liquid that was trapped in the inclusions during crystallization that invaded the inclusion during eruption. Unfortunately, textures alone do not distinguish cognate precipitates from the precipitates of an earlier melt which were later incorporated by a different magma. In this study the phenocrysts are useful in making this distinction.

The cores of the small, zoned phenocrysts of augite in the limburgite have the same composition as the clinopyroxene of the inclusions, while the rims of these phenocrysts have the same composition as the groundmass augite in the limburgite. This suggests that the inclusions are cognate precipitates, but the proof is inconclusive, because the cores of the augite phenocrysts in the limburg-

---

EXPLANATION OF PLATE 5
PHOTOMICROGRAPHS OF INCLUSIONS

FIG. 1.—Amphibole-phlogopite clinopyroxene from northwest segment of dike. Light grains along margins of photograph are augite (c), dark sinuous bleb of phlogopite (p) is jacketed by anhedral amphibole (a). Void in upper left is plucked grain. Inclusion is 3 cm. across.

FIG. 2.—Ovoidal cavity of $CaCO_3$ at the junction of mica and pyroxene grains in inclusion C of diatreme 2. Darker areas are serpentine; regions outlined in ink are unidentifiable mineral which has moderate relief and low second order interference colors.

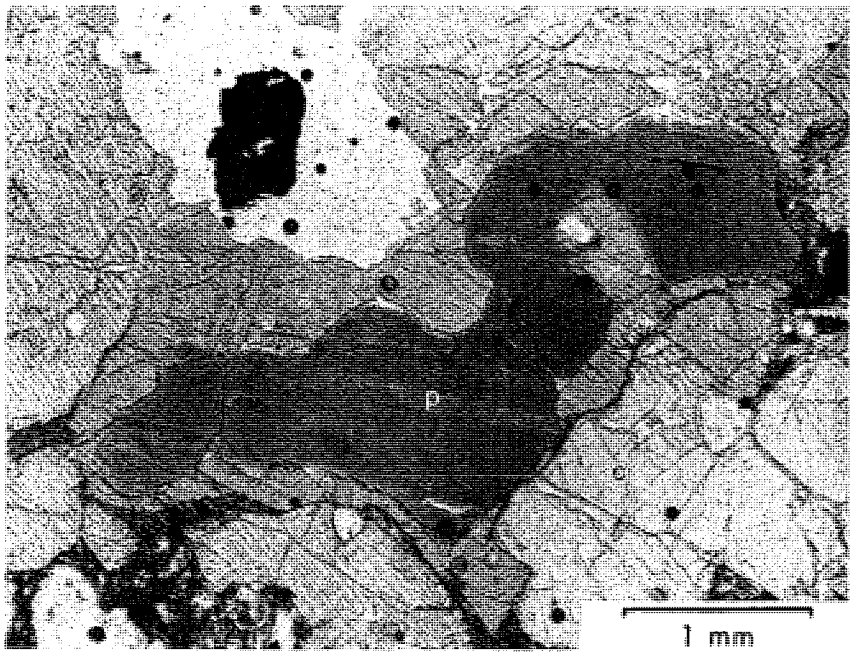

1

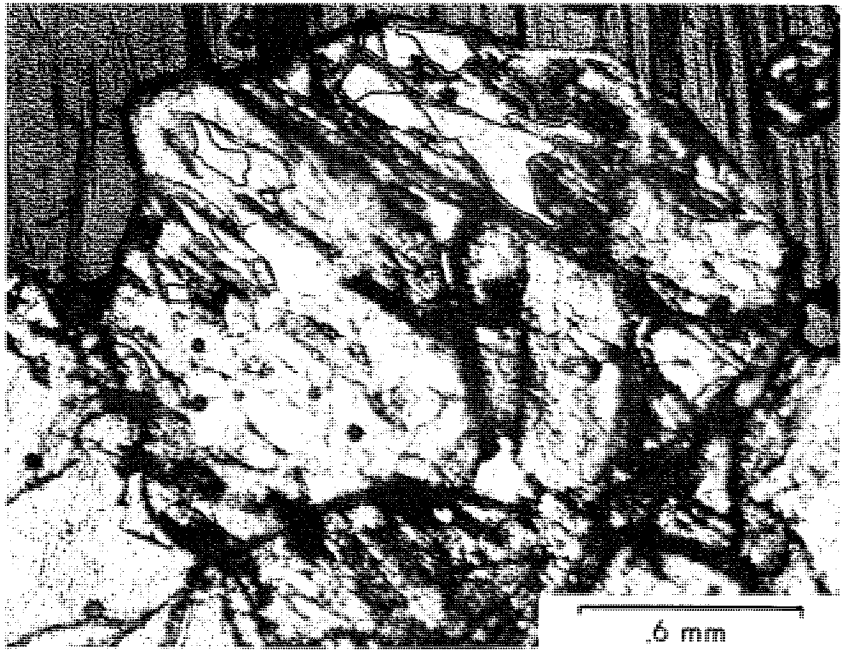

2

PLATE 5

ite could represent fragments derived from disintegrated megacrysts or inclusions that crystallized from an earlier melt and then zoned with more pyroxene of the "new" host melt.

It is believed that the large euhedral, unzoned phenocrysts of the tuff are cognate to the limburgite melt that produced the eruption. If they were the product of an earlier melt, the likelihood of disaggregation, resorption, or additional precipitation by the limburgite melt would preclude the euhedral shape and lack of zoning which is observed. That the unzoned phenocrysts in the tuff are genetically related to the clinopyroxene of the inclusions and the megacrysts is suggested by their overall chemical similarities. As an example, consider the distribution of aluminum in the clinopyroxene molecular formula. White (1964) and Aoki, et al. (1968) have utilized a plot of octahedral aluminum versus tetrahedral aluminum in clinopyroxene in order to relate the mineral to the petrological suite from which it comes. Text-figure 7 shows the

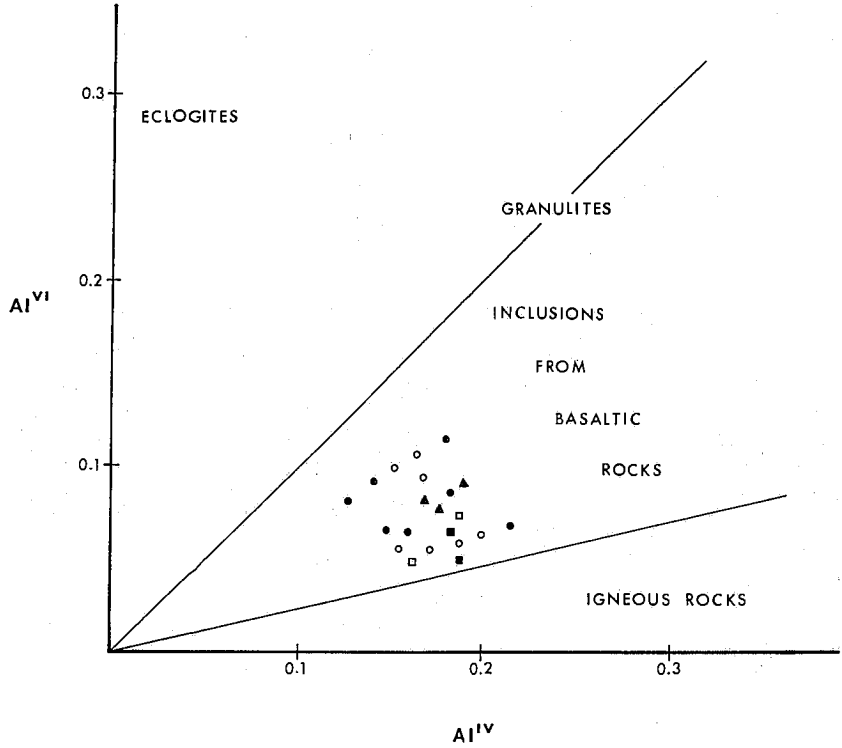

TEXT-FIGURE 7.—Octahedral versus tetrahedral aluminum in clinopyroxene based on six oxygens and molecular formulae, after Aoki and Kushiro (1968). Rock types from which various clinopyroxenes originate are labeled. The lower line marks the boundary between clinopyroxenes from igneous rocks and those from inclusions of basaltic rocks. The upper line marks the position of the Ca-Tschermak molecule in clinopyroxene. Solid circles are clinopyroxenes from the dike inclusions; open circles are clinopyroxenes from the inclusions of diatreme 2; solid triangles are the clinopyroxene megacrysts; open squares are the large euhedral nonzoned augite phenocrysts from the tuff; and the solid squares are the cores of the small zoned augite phenocrysts from the limburgite.

plot of the clinopyroxenes of the inclusions, megacrysts, and phenocrysts. The close relation of the clinopyroxene from these various occurrences is obvious. These and the preceeding data all point to a common origin for the inclusions, megacrysts, and phenocrysts. Therefore, if the large euhedral, unzoned phenocrysts from the tuff are correctly interpreted as being cognate to the limburgite melt that generated the eruption, the inclusions and megacrysts are also cognate precipitates.

The presence of small, zoned augite phenocrysts in the limburgite and large, unzoned ones in the tuff probably reflects the rapidity, i.e., the explosiveness, of the eruption which produced the latter rock type.

Although many variation diagrams may be drawn, significant trends are evident in the MgO, FeO, and Na_2O for clinopyroxene (Text-fig. 6). Conclusions which can be drawn from this diagram are two:

1. The inclusions, phenocrysts, and megacrysts form a suite which has an expected magmatic variation of higher Na_2O with lower Mg/Fe ratio.
2. The large euhedral, unzoned phenocrysts fit into these trends and were probably derived from a melt compositionally similar to, if not the same as, those which produced the inclusions and megacrysts.

ORIGIN OF LIMBURGITE MELT

The data and conclusions heretofore presented can now be used in investigating fractionation trends, i.e., the role of fractionation, in the genesis of the limburgite melt and any possible genetic relation between the limburgite and monchiquite of the field.

To determine fractionation trends in the limburgite melt, the data are used to compute hypothetical parental melts of the limburgite. Interpreting the inclusions and megacrysts as cognate precipitates at high pressures permits the calculation of such parental melts if contamination of the residual melt has not occurred. Rapid ascent of the melt is ascertained by the specific gravity of the inclusions (3.1-3.2), a fact which virtually precludes contamination above the region where the inclusions were formed (Green, 1969). Mixing with another magma during ascent is possible but is considered improbable. The reasonably uniform distribution of megacrysts and inclusions in the dike would necessitate thorough mixing of the inclusion-bearing magma with the contaminate. Such thorough mixing would presumably require a fairly lengthy period of time during which the denser materials could settle out and be partially to totally resorbed in their new environment.

The amount of precipitation of megacrysts and inclusions prior to eruption is not known, so two parental liquids of the limburgite magma are computed on the basis of 10 and 50% crystallization (Table 13). The dike host rock is used for these computations. The two parental liquids were determined by using an "average" inclusion-megacryst assemblage consisting of 80% clinopyroxene, 15% phlogopite, and 5% amphibole. Average compositions for the inclusion phases were computed from the data on both the dike and diatreme 2 to compensate partially for the changing composition of the crystal accumulate as crystallization proceeded. The questionable appearance of orthopyroxene in the crystallization sequence does not justify using it in computing parental liquids.

TABLE 13
PARENTAL MELTS OF LIMBURGITE

	1	2	3	4
SiO_2	42.50	42.95	44.77	40.89
TiO_2	3.69	3.56	3.06	3.77
Al_2O_3	12.21	11.75	9.90	12.28
FeO	12.74	12.26	10.31	12.47
MnO	0.40	0.38	0.28	0.17
MgO	7.92	8.59	11.25	12.83
CaO	13.58	13.83	14.86	12.37
Na_2O	3.61	3.39	2.53	3.19
K_2O	1.11	1.16	1.34	0.45
P_2O_5	1.53	1.38	0.77	1.08
Total	99.29	99.25	99.07	99.50
or	6.56	5.56	0.56	
lc		0.31	4.66	1.93
ab	4.50			
ne	13.83	15.57	11.31	14.12
cs				0.84
an	13.82	22.21	20.08	27.72
di	33.40	27.34	38.06	16.31
ol	15.62	17.72	17.08	28.27
il	7.05	6.83	5.77	7.14
ap	4.06	3.61	1.85	2.96

1 - Limburgite, dike, see Table 3. 2 - Parental melt comprised of 10% inclusions + limburgite liquid. 3 - Parental melt comprised of 50% inclusions + limburgite liquid. 4 - Typical monchiquite from Hopi Buttes field, recalculated to water-free composition with total iron as FeO (Williams, 1936). This composition is in essential agreement with preliminary atomic absorption analyses on six samples from three different localities.

The fractionation trends involving the limburgite and parental melt compositions in Table 13 should be meaningful in interpreting chemical variations in the limburgite from one locality to the next, if fractionation, indeed, did play an important role in the development of the Hopi Buttes field. However, comparison of the limburgite from different localities (Table 3) shows that the compositional variations in the limburgite do not conform to the expected fractionation trends. This indicates that fractionation has not been important in the genesis of the limburgite, and that each locality of limburgite may possibly have originated from an independent magma.

The reasoning used above can be employed to test for any correlation between the limburgite and monchiquite. Monchiquite is widespread in the plugs and flows of the Hopi Buttes field, and its representative composition is listed in Table 13. Volumetrically, monchiquite is much more abundant than limburgite, a fact which, by itself, suggests that if the two rock types are genetically related then the monchiquite would have been the parental melt of the limburgite. Table 13 shows that the monchiquite could not yield the limburgite by fractionation of the inclusion phases, nor vice versa. Thus, the monchiquite and limburgite are not related by any means of fractionating simple phase combinations.

The above conclusion, together with a comparison of the limburgite and monchiquite compositions with those of expected partial melts of mantle peridotite (Green and Ringwood, 1967; Keisuke and Kennedy, 1967; and Kushiro et al., 1968), reveals that both rock types could have derived from separate batches of partial melt. The monchiquite is compatible with expected partial melts of the mantle, and the limburgite could be produced by partial

melting if the degree of partial melting was very low. Low degrees of partial melting produce an initial liquid rich in alkalis and low in magnesium. The degree of partial melting needed to produce the different compositions also correlates very well with the relative volume of the two rock types in the field.

CONCLUSIONS

Conclusions which can be drawn as a result of this project are:

1. Limburgite of the dike and diatremes is rich in titanium, sodium, and calcium.
2. Inclusions and megacrysts are cognate precipitates that were probably crystallized at high pressures. Fractionation of inclusion and megacryst phases was probably not extensive enough to create the observed chemical variation in the limburgite.
3. Inclusions were probably derived from a clinopyroxenite body of minimal thickness underlying the dike and diatreme 2. This body is probably not continuous beneath the limburgite localities of the Hopi Buttes field.
4. There is no apparent genetic connection between the abundant monchiquite of the field and the limburgite, and no fractionation of simple phase combinations can produce one from the other.
5. The limburgite and monchiquite have most likely originated from distinct batches of partial melts from the mantle.
6. Since the inclusions are apparently of igneous origin and are also cognate with limburgitic liquids, it becomes very obvious that a marked inadequacy exists between the phase relations observed in natural, hydrous, alkalic, basaltic systems and available experimental data. The experimental data is neither adequate nor extensive enough to begin to account for the suite of clinopyroxene-phlogopite-amphibole inclusions herein discussed. This would suggest a more practical approach in laboratory investigations and a renewed effort in better simulating natural environments, particularly those of high alkali and water content.

REFERENCES CITED

Aoki, K., and Kushiro, I., 1968, Some clinopyroxenes from ultramafic inclusions in Dreiser Wheiher, Eifel: Contr. Mineral. Petrol., v. 18, p. 326-337.

Binns, R. A., Duggan, M. B., and Wilkinson, J. F. G., 1970. High pressure megacrysts in alkaline lavas from Northeastern New South Wales: Amer. Jour. Sci., v. 269, p. 132-168.

Brimhall, W. H., and Embree, G. F., 1971 Rapid analysis of basalts by atomic absorption spectrophometry: Brigham Young Univ. Geol. Stud., v. 18, no. 3, p. 123-130.

Bultitude, R. J. and Green, D. H., 1967, Experimental study at high pressures on the origin of olivine nephelinite and olivine melitite nephelinite magmas: Earth Planet. Sci. Letters, v. 3, p. 325-337.

———, 1971, Experimental study of crystal-liquid relationships at high pressures in olivine nephelinite and basanite composition: Jour. Petrol., v. 12, p. 121-147.

Clark, S. P., Schairer, J. F., and de Neufville, J., 1962, Phase relations in the system $CaMgSi_2O_6$—$CaAl_2SiO_6$—SiO_2 at low and high pressure: Carnegie Inst. Wash., Year Book 61, p. 59-68.

Deer, W. A., Howie, R. A., and Zussman, J., 1963, Rock forming minerals: Vol. 2, chain silicates: Longmans, Green and Co. Ltd., 379 p.

———, 1966, An introduction to the rock-forming minerals: John Wiley and Sons, Inc., 538 p.

Gilbert, M. C., 1969, Reconnaissance study of the stability of amphibole at high pressure: Carnegie Inst. Wash., Year Book 67, p. 167-170.
Green, D. H., 1969, The origin of basaltic and nephelinitic magmas in the earth's mantle: Tectonophysics, v. 7, p. 409-422.
———, 1970, A review of experimental evidence on the origin of basaltic and nephelinitic magmas: Phys .Earth Planet. Interiors, v. 3, p. 221-135.
———, and Hibbersion, W., 1970, Experimental duplication of conditions of precipitation of high pressure phenocrysts in a basaltic magma: Phys. Earth Planet Interiors, v. 3, p. 247-254.
———, and Ringwood, A. E., 1967, The genesis of basaltic magmas: Contr. Mineral. Petrol., v. 15, p. 103-190.
Hack, J. T., 1942, Sedimentation and volcanism in the Hopi Buttes, Arizona: Geol. Soc. Amer., Bull., v. 53, p. 335-372.
Higazy, R. A., 1954, Trace elements of volcanic ultrabasic potassic rocks of Southwestern Uganda and adjoining part of the Belgian Congo: Geol. Soc. Amer., Bull., v. 66, p. 39-70.
Holmes, A., 1950, Petrogenesis of katungite and its associates: Amer. Mineral., v. 35, p. 772-792.
Ishibashi, K., 1970, Petrochemical study of basic and ultrabasic inclusions in basaltic rocks from northern Kyushu, Japan: Mem. Fac. Sci., Kyushu Univ., Ser. D. Geology, v. 20, p. 85-146.
Ito, K., and Kennedy, G. C., 1968, Melting and phase relations in the plane tholeiite-lherzolite-nepheline basanite to 40 Kb with geological implications: Contr. Mineral. Petrol., v. 19, p. 177-211.
Keisuke, I. and Kennedy, G. C., 1967, Melting and phase relations in a natural peridotite to 40 Kb: Amer. Jour. Sci., v. 265, p. 519-538.
Kuno, H., 1964, Aluminum augite and bronzite in alkali olivine basalt from Takasima, North Kyushu, Japan: Advancing Frontiers in Geol. and Geophys., p. 205-220.
Kushiro, I., 1960, Si-Al relations in clinopyroxenes from igneous rocks: Amer. Jour. Sci., v. 258, p. 548-554.
———, 1962, Clinopyroxene solid solutions, Part I. The $CaAl_2SiO_6$ component: Japan Jour. Geol. Geogr., v. 33, p. 213-220.
———, 1965, Clinopyroxene-solid solutions at high pressures: Carnegie Inst. Wash., Year Book 64, p. 112-117.
———, 1969, Stability of amphibole and phlogopite in the upper mantle: Carnegie Inst. Wash., Year Book 68, p. 245-247.
———, Syono, Y., and Akimoto, S., 1968, Melting of a peridotite nodule at high pressures and high water pressures: Jour. Geo. Res., v. 73, p. 6023-6029.
Leake, B. E., 1968, A catalog of analyzed calciferous and subcalciferous amphiboles together with their nomenclature and associated minerals: Geol. Soc. Amer. Spec. Paper 98, 210 p.
LeBas, M. J., 1962, The role of aluminum in igneous clinopyroxenes with relation to their parentage: Amer. Jour. Sci., v. 260, p. 267-288.
Lowell, J. D., 1956, Occurrence of uranium in Seth La Kai diatremes, Hopi Buttes, Arizona: Amer. Jour. Sci., v. 254, p. 404-412.
McGetchin, T. R., 1968, The Moses Rock dike: Geology, petrology and mode of emplacement of a kimberlite-bearing breccia dike, San Juan County, Utah: unpublished Ph. dissertation, California Institute of Technology, Pasadena, 440 p.
Naeser, C. W., 1971, Geochronology of the Navajo-Hopi diatremes, Four Corners area: Jour. Geol. Res., v. 76, p. 4978-4985.
Nicholls, J. W., 1969, Studies of the volcanic petrology of the Navajo-Hopi area, Arizona, unpublished Ph.D. dissertation, Univ. Calif., Berkeley, 114 p.
Nicholls, J., Carmichael, I. S. E., and Stormer, J. C., Jr., 1971, Silica activity and P *total* in igneous rocks: Contr. Mineral. Petrol., v. 33, p. 1-20.
Roedder, E., 1965, Liquid CO_2 inclusions in olivine-bearing nodules and phenocrysts from basalts: Amer. Mineral., v. 50, p. 1746-1782.
Rucklidge, J. C., 1967, A computer program for processing microprobe data: J. Geol., v. 75, p. 126.
———, Gibb, F. G. F., Fawcett, J. J., and Gasparrini, E. L., 1970, Rapid rock analysis by electron microprobe: Geochim. et Cosmochim. Acta, v. 34, p. 243-247.
Shoemaker, 1955, Occurrence of uranium in diatremes of the Navajo and Hopi reservations, Arizona, New Mexico, and Utah: U. S. Geol. Survey Prof. Paper 300, p. 179-185.

Waters, A. C., 1955, Volcanic rocks and the tectonic cycle: Geol. Soc. Amer. Spec. Paper 62, p. 703-722.
Watson, K. D., 1967, Kimberlite pipes of Northeastern Arizona: *in* Ultramafic and Related Rocks, P. J. Wyllie [ed], Wiley and Sons, Inc.
White, A. J., 1964, Clinopyroxenes from eclogites and basic granulites: Amer. Mineral., v. 49, p. 883-888.
Wilshire, H. G., and Trask, N. J., 1972, Structural and textural relations of amphibole and phlogopite in peridotite inclusions, Dish Hill, California: Amer. Mineral., v. 56, p. 240-255.
Williams, H., 1936, Pliocene volcanoes of the Navajo-Hopi country: Geol. Soc. Amer., Bull., v. 47, p. 111-172.
Yoder, H. S., Jr., 1969, Phlogopite—H_2O—CO_2: An example of the multicomponent gas problem; Carnegie Inst. Wash., Year Book 68, p. 236-240.
———, and Kushiro, I., 1969, Melting of a hydrous phase: Phlogopite: Amer. Jour. Sci., v. 267-A, p. 558-582.